UNIVERSITY OF TARTU

Faculty of Science and Technology

Institute of Physics

Chinedu Henry Ofoegbu

CAPACITIVE BEHAVIOUR OF ATOMIC LAYER DEPOSITED NANOMATERIALS FOR MEMORIES

Master's Thesis (30 ECTS)

Curriculum Material Science and Technology

Supervisors:

KAUPO KUKLI, PhD

JOONAS MERISALU, MSc

JANUARY 2022

ABSTRACT

This research was devoted to the capacitive behavior of thin solid films, which consisted of zirconium and aluminum oxide layers alternately grown as stacked structures by atomic layer deposition technique. The materials were chosen as those applied in contemporary dynamic random access memory chips. The study was carried out in order to examine whether the charge storage ability of the capacitors built on such materials, expressed by the measured capacitance and calculated relative dielectric permittivity of the oxide film material, can be enhanced after appropriate modification of the atomic layer deposition cycle sequences for both constituent metal oxides. The results were expected to add to the knowledge about the interrelationship between structural ordering, i.e., crystallization, content of aluminum dopant and average dielectric permittivity. The improved dielectric performance might assist in further studies leading to nonvolatile resistive switching memory materials.

In the present study, 10-20 nm thick nanocrystalline zirconium oxide – aluminum oxide capacitor dielectrics were grown by atomic layer deposition at 300 ^{o}C from zirconium tetrachloride, trimethylaluminum, and water, as the precursors. The electrical measurements revealed that the deposition cycle sequences modified to change the aluminum content and, concurrently, structural order allowed one to dramatically change the average permittivity. Very generally, the capacitance and permittivity of the films between titanium nitride and titanium electrodes increased with the decrease in the aluminum content. In samples where the crystallization was increased, the permittivity values could exceed approximately 1.5 and 2 times those characteristic of reference zirconium and aluminum oxides, respectively.

CERCS codes:
P260 Condensed matter: electronic structure, electrical, magnetic and optical properties, supraconductors, magnetic resonance, relaxation, spectroscopy

T150 Material technology

ABSTRAKT EESTI KEELES

Uurimistöö oli pühendatud õhukeste tahkiskilede mahtuvusliku käitumise uurimisele. Kiled koosnesid tsirkooniumi ja alumiiniumi oksiidi kihtidest, mis olid vaheldumisi sadestatud tahkete korrusstruktuuridena aatomkihtsadestamise meetodil. Materjalid olid valitud vastavalt tänapäevastes dünaamilistes arvutimuutmälukiipides kasutatavatele. Töid viidi läbi uurimaks seda, kas sellistele materjalidele ehitatud kondensaatorite laengusäilitamise võimet, mis suhestub mõõdetud mahtuvuse ja selle baasil hinnatud oksiidmaterjali suhtelise dielektrilise läbitavusega, võiks suurendada pärast mõlema koostisoksiidi aatomkihtsadestamise tsüklite järgnevuste modifitseerimisega. Töö tulemustest oodati uusi teadmisi selle kohta, kuidas suhestuvad omavahel materjali struktuurne korrastatus ehk kristallilisus, alumiiniumlisandi hulk oksiidmaterjalis ning keskmistatud dielektriline läbitavus. Parendatud dielektrilised omadused võiksid edaspidi olla kasulikud töödes, mis on suunatud takistuslülituvate püsimälude komponentmaterjalide arendamisele.

Käesolevas töös aatomkihtsadestati 10-20 nanomeetri paksused tsirkooniumi ja alumiiniumi oksiididest koosnevad kondensaatordielektrikukiled 300 ^{o}C juures tsirkooniumi tetrakloriidist, trimetüülalumiiniumist ja veest kui lähteainetest. Elektrimõõtmised näitasid, et alumiiniumi sisalduse ning struktuurse korrastatuse reguleerimiseks kasutatud sadestustsüklite järgnevuste muutused võimaldasid märkimisväärselt muuta dielektrilist läbitavust. Üldistatult – titaannitriidist ja titaanist elektroodide vahele formeeritud oksiidkilede mahtuvus ja läbitavus suurenesid koos alumiiniumi sisalduse kahanemisega. Nendes prooviobjektides, kus kristallisatsioon oli tuvastatult intensiivsem, ületasid dielektrilise läbitavuse väärtused ligikaudu 1.5 ja 2 korda vastavalt ainult tsirkooniumi oksiidist ja ainult alumiiniumi oksiidist formeeritud võrdlusobjektidele karakteristlikke väärtusi.

(CERCS) teadusvaldkondade ja -erialade klassifikaator:

P260 Tahke aine: elektrooniline struktuur, elektrilised, magneetilised ja optilised omadused, ülijuhtivus, magnetresonants, spektroskoopia

T150 Materjalitehnoloogia

TABLE OF CONTENTS

1. INTRODUCTION

1.1 MEMORY CAPACITORS AND THE CHALLENGES IN THEIR DEVELOPMENTS

Nanoelectronic devices, that is memory capacitors and transistors constitute all emerging generations of integrated circuits. Continuous research and development of component materials in electronic switches and memory cells is required because innovation is essential to meet up with the continuous demand for higher speed, better performance, reliability and extra-low reading, writing or switching voltages. Attempts have been made by several hardware companies such as Samsung, IBM, Motorola and others to deploy more and more simplified memory cell structures consisting of transistor and capacitor in a single dynamic random access memory (DRAM) cell structures. The development has led to accommodation of earlier established synthesis routes, in particular, atomic layer deposition (ALD) to ultrathin (1-10 nm) solid films of high permittivity (high-k) metal oxides for capacitor dielectrics.

Exploration of memory stacks with nanocrystalline ZrO_2 or amorphous Al_2O_3 as single dielectric layers have indicated that the performance of devices may not be sufficiently easily optimized due to high current leakage through dielectrics, especially, in the negative bias that is, electron current injected from top metal electrodes. Further research, which showed results of industrial value, indicated the usefulness of depositing stacked oxide layers, i.e., ultrathin (1 nm and less) Al_2O_3 layers between ZrO_2 host films [Cho, 2006, IEEE Conf.; Cho, 2007, Solid-State Electr.]. In this way, insertion of Al_2O_3 enabled stabilization of even higher permittivity ZrO_2 phases and accompanying higher capacitance of the memory capacitor. Secondly, the Al_2O_3 layer created additional inner barriers against electronic leakage currents, accompanied with longer retention of the charge stored on capacitor. Thus, improvements were made and materials with high-permittivity (so-called high-k) dielectric introduced, in order to reduce the electrical thickness without altering the physical thickness. These developments, although not yet necessarily sufficient enough, have led to an upward surge in the market value of the semiconductor market around the word. The demand for increased speed at a low cost while maintaining a reduced size is only achievable at the moment using a transistor CMOS, and ALD technique.

1.2 EXISTING AND EMERGING APPLICATIONS OF ATOMIC LAYER DEPOSITION (ALD) IN ELECTRONICS

Atomic layer deposition is a nanotechnology-based deposition process employed for growing very thin films on substrates of any shape and geometry. The two distinct characteristics of atomic layer deposition are highly conformal and self-limiting atomic layer by layer growth [Hausmann 2002, Chem. Mater.]. With controlled temperature on deposition surface where the alternate saturative adsorption and reaction of two precursors result in self-limiting submonolayer-by-submonolayer film growth, thus providing nanometric, dense, both structurally and compositionally uniform films on large-area, technologically relevant, wafer substrates [Xie, 2020, Coatings]. The gate dielectric oxides in processor transistors were changed from SiO_2 to HfO_2, and dielectric insulator layers of capacitors in memory chips from Al_2O_3 eventually to ZrO_2, both manufactured by atomic layer deposition [Hwang and Yoo, 2014].

Apart from depositing the functional material layers inside the integrated circuit component, the method has also been widely used in electronic device manufacturing to deposit barrier layers protecting against moisture impurities and oxygen, prolonging the lifetime and failure free operation upon fabrication of electronic components for processor and memory chips [Hwang and Yoo, 2014]. ALD has, in that way, also been used for producing special oxide films besides high dielectric constant insulators, e.g., oxide films with inter-poly dielectric oxide, films blocking oxide, adhesion layer films for ferromagnetic materials, diffusion barrier films et cetera.

In the context relevant to the present work, it is important to note, that ALD has earlier been successfully used in growing several MIM dielectric such as Al_2O_3, TiO2, Ta_2O_5, ZrO_2, HfO_2 [Clark, 2014, Materials; Kukli, 2007, Microel. Eng.].

In dynamic random access memory capacitors manufacturing, the main advantages of atomic layer deposition over other gas phase deposition techniques include precise film thickness control which is achievable by simply changing the number of deposition cycles even without controlling the dose of the precursor. Uniform doping, when necessary, is easy to accomplish by replacing the growth cycle by a doping cycle at the desired interval.

1.3. ZIRCONIUM OXIDE AND ITS APPLICATION IN DYNAMIC RANDOM ACCESS MEMORY.

When the minimum feature sizes of DRAM capacitors, upon following the development trends, shrinked to sub 80nm technology generations, high permittivity (high-k) dielectric materials became intensely investigated in order to find a replacement for Al_2O_3 as capacitor dielectrics in MIM capacitors [Cho, 2007, Solid-State Electr.], whereby the insulating properties of Al_2O_3 remain superior to that of ZrO_2 and HfO_2,

Thereby it is important to remember, that both HfO_2 and ZrO_2 are termed, on such a background, high-permittivity oxides compared to the property of their predecessors, SiO_2 and Al_2O_3, respectively. The dielectric permittivities of amorphous SiO_2 and Al_2O_3 remain at

3.9 and 7-9, respectively. The measured dielectric permittivity of nanocrystalline HfO_2 and ZrO_2 can reach, depending on the phase stabilized, 17-20, and 25-40, respectively.

ZrO_2 has been and can still be investigated as potential gate dielectric material for thin film field effect transistors [Xie, 2020, Coatings]. This might succeed, if the transistors have to be fabricated on flexible polymer substrates and high channel activation temperatures are not allowed due to the sensitivity of the substrate material. However, in the case of silicon-based electronics, the gate dielectric oxide (either ZrO_2 or HfO_2) must stand against high-temperature (over 1000 Celsius degrees) heat-treatment, and they also must not strongly become intermixed with Si substrate under heating in ovens. Along with such experiments, it has long time (over 20 years) ago come out that the chemical stability of ZrO_2 grown on Si remains inferior to the stability of HfO_2, which was most probably the reason why HfO_2 has become the gate dielectric insulator chosen for contemporary processor transistors. At approximately the same time, ZrO_2 stood out as a material akin to HfO_2 which still was **a)** chemically less stable when deposited on silicon transistor channel, compared to HfO_2; and **b)** was relatively easily stabilized in higher-permittivity tetragonal or cubic forms, compared to monoclinic HfO_2. Since the production of memory capacitors does not require heat-treatments at the same level as transistors do, ZrO_2 did "win the competition", and became the basic dielectric insulator material still used in DRAM chips.

Zirconium dioxide (zirconia, ZrO_2) is, in its bulk form, a white crystalline material. Its most naturally occurring form is the monoclinic crystalline structure. Herewith it is important to memorize, that the zirconia films, if crystallized into monoclinic ZrO_2 phase can possess relative dielectric permittivity not exceeding 20 at frequencies relevant to microelectronics (10 kHz – 1 MHz). The zirconium oxide phases other than that of monoclinic can be stabilized quite reliably in thin solid films. In this case, the metastable forms of zirconia, that is cubic and tetragonal ZrO_2 phases, possess markedly higher permittivity, which may reach up to 40, depending on the adjustment of the crystal growth in the nanocrystalline metal oxide layers.

In an industrial scale, a significant memory manufacturer (Micron) chose switching from HfO_2 as the memory capacitor dielectric to ZrO_2 [Wintgens, 2009, EETimes], because ZrO_2 possesses somewhat higher dielectric permittivity and demonstrates, as claimed, lower leakage currents compared to those of HfO_2. Nowadays, ZrO_2 is the main constituent material in DRAM cells. DRAM manufacturers have been enforced to target the maximum capacitance of the storage capacitor design without strong modifications in physical size and topology of the capacitors.

1.4. CURRENT RESEARCH ON VARIOUS FORMS OF ZrO_2 BASED MEMORY CAPACITORS, RESISTIVE SWITCHING MEMORIES

The studies of capacitive properties of ZrO_2-based solid films layers naturally and at first relate to the volatile memory capacitor materials. The information bits stored on such memory capacitors, when used in computers, are to be periodically refreshed, meaning that they have to be recharged in order to maintain the bit. This is typical for dynamic random access memories, DRAM's, which consist of memory cell matrixes, in which each cell can be addressed individually. Nonetheless, it has come out, that ZrO_2-based solid films can also exhibit properties which might enable their exploitation in non-volatile (permanent) memory structures. In such cases the capacitance is not the primary characteristic of the memory cell, but the information bits are distinguished on the basis of two different conductivity or specific resistivity states alternately switchable in the solid film material. Such effect or behavior is called resistive switching. Examination of resistive switching in ZrO_2-based films remains beyond the scope of the present thesis work. However, the same research objects will further be investigated as possible resistively switching media. Herewith the characterization of capacitive properties is important, because the capacitance and dielectric permittivity are related to film density and structure, affecting the electrical current conduction and material's resistivity. This justifies briefing of resistive switching effect, as follows.

Resistive switching refers to the physical phenomena where a dielectric suddenly changes its resistivity under the influence of a strong electrical field or current. Resistively switching films are materials, which are basically insulating dielectrics, but inherently defective whereby the defect densities is controlled and stabilized at some levels. Change (switching) in material's resistivity, initially from high resistivity state to low resistivity state, is non-volatile and reversible. The resistivity states can be reversed from low to high resistivity by applying even stronger electrical field (so-called unipolar switching mechanism), or by applying electrical field of opposite direction, i.e., voltage with opposite polarity on electrodes (bipolar switching mechanism). Typical resistive switching systems are capacitor-like devices, where the electrodes are usually made of some metal and the dielectric is most commonly some transition metal oxide. Similarly, to capacitive cells in DRAMs, the resistively switching cells are to be arranged in chips in the form of matrix, in which all cells can be addressed independently and directly. Such memories can then be called resistive switching random access memories (RRAM) and few companies may already have become able to actually produce corresponding chips [Hua, 2019, Adv. Sci.]

The next generation non-volatile resistive switching memories still have shortcomings related to the control of oxygen vacancies, which form the conductive path in the materials. Various approaches related to the selection of materials, doping, and thermal treatments have been attempted to achieve stable resistive switching behavior. For instance, the research on effects of thermal treatment may require particular efforts in order to improve the switching characteristics of the devices [Y. Abbas, 2019, J. Mater. Sci.]. Zirconium oxide has already attracted considerable attention due to its potential application RRAM devices, all due to their simple structure, high memory bit density, and nondestructive reading of

the stored information [Panda, 2013, Thin Solid Films; T. Kahro 2020, J. Vac. Sci. Tech.; Y. Abbas, 2019, J. Mater. Sci].

Expectedly, several issues are connected to the ZrO_2 based RRAM devices, including high operation voltage, low ratio between low and high resistivity states, and high-voltage forming process, which are still to be improved in order to ensure ZrO_2-based RRAM behavior, satisfying the demands before practical nonvolatile memory applications. While exploring the influence of the composition of Al/Ti/ZrO_2:Al_2O_3/TiN/Si/Al structures on the switching behavior, Castán *et al*. [Castán, 2018, ECS Trans.] have concluded that the composition of dielectrics has clear influence on the range of switching voltage values.

1.5. THE AIM OF THESIS

The aim of the present Thesis work was to study the capacitive behavior of atomic layer deposited nanomaterials in the form of zirconium oxide films containing aluminum oxide as a dopant. To undertake this research, 10-20 nm thick ZrO_2 films doped with Al_2O_3 layers were investigated. Two types of the films as research objects were prepared: a) periodical layering of ZrO_2 and Al_2O_3, and b) deposition of ZrO_2 on ZrO_2:Al_2O_3 buffer layers. Such structures were fabricated and studied for the first time. The goal of the work was to examine and prove the positive effect of the doping on the nanocrystalline phase formation and accompanying advancement in the capacitive properties of nanolayers in terms of dielectric permittivity.

2. MATERIALS AND METHODS

2.1 CAPACITORS AND THE REPRESENTATION OF CAPACITANCE

A Capacitor is a simple device which store energy in the form of electrical charge. It consists of two parallel plates made of conductors which are electrically separated by a non-conductor, forming a sandwiched structure consisting of two electrodes and dielectric insulator between them [Grove, 2005, Am. J. Phys.]. The non-conductive item between the plates is called a dielectric. The capacitors ability to hold electrical charges, i.e., the capacitance is a function of the surface area of the parallel electrode plates, the distance between the plates, and the dielectric constant (actually relative permittivity of the solid material). The capacitance in farads is expressed by the parallel plate capacitor formula as follows:

$$C = \varepsilon\, \varepsilon_0 \frac{A}{d}$$

Where C = capacitance of the capacitor,
A = the surface area of the plates, in square meters,
d = the distance between the plates, in meters
ε = the permittivity of the dielectric material, and
ε_0 = permittivity of vacuum, $8.854 \cdot 10^{-12}\ CV^{-1}m^{-1}$, a constant.

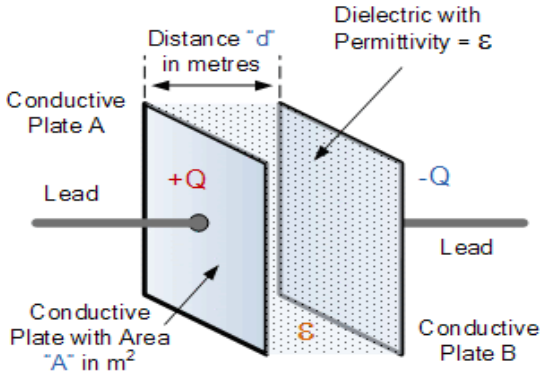

Figure 1 - Capacitor represented by two parallel plates.
Adapted from https://www.electronics-tutorials.ws/capacitor/cap_1.html

2.2 CAPACITANCE AND THE DIELECTRIC MATERIAL.

The capacitance of a parallel plate capacitor fundamentally depends on the surface area of the conductive plates and the distance between them. Another factor which affects the overall capacitance of the device is the type of dielectric material being used. The main property of such a material is referred to as the relative permittivity (**ε**) of the dielectric medium, for instance, ZrO_2 [Huang, 2005, J. Vac. Sci. Tech.]. From the point of view of physics and engineering, the permittivity is the measure to that how many times the electric field applied to the material layer is decreased in the material, compared to the external field strength. Alternatively, one may state, that the permittivity of a material is a factor by which the solid dielectric material increases the capacitance of the capacitor compared to air. In other words, relative permittivity is a measure of resistance encountered when creating an electric field in solid medium.

It is worth noting that in the case of very well defined crystal structure of a (monocrystalline) material, the permittivity of such a material has been and may still be termed as dielectric constant, also in the case of ZrO_2 [Harrop and Wanklyn, 1967, Brit. J. Appl. Phys.]. Dielectric constant is, then, dependent on lattice orientation, and in the case of polycrystalline material, e.g. ZrO_2, one can probably count on orientationally averaged dielectric constant [Zhao and Vanderbilt, 2002, Phys. Rev. B]. Moreover, even an amorphous material, exemplified again by ZrO_2, has been characterized by dielectric constant [Zhao, Cerezoli, and Vanderbilt, 2005, Phys. Rev. B]. However, the term constant may as well remain confusing, because in real, disordered, thin film materials the polarization can exhibit strong dispersion, i.e. dependence on measurement frequency [Wilk, Wallace, and Anthony, 2001, J. Appl. Phys.]. Besides, the polarization in real deposited materials depends on structural (dis)order, changing strongly with the degree of crystallinity and also with the chemical purity. As these properties cannot possibly be regarded as constant values, it will probably be less confusing to further exploit the term "relative permittivity". In any case, a dielectric material with higher dielectric constant (permittivity) is a better capacitor dielectric material than a material with a lower dielectric constant (permittivity), because it provides higher charge storage [Grove, 2005, Am. J. Phys.].

2.3 ESTIMATION OF THE PERMITTIVITY OF DIELECTRIC MATERIALS

The capacitance measurements are commonly carried out by applying some voltage on capacitor plates. If there were no dielectric material between the capacitor plates, then the permittivity calculated from the measured capacitance would be that of free space, represented as $\boldsymbol{\varepsilon_o}$. Once an insulating material (dielectrics) is inserted between the plates the permittivity will change accordingly. Dielectric insulators should not contain free moving charge carriers, as metals do, but they do contain positive nuclei and negative electrons [Grove, 2005, Am. J. Phys.]. These may be arranged along the lines of an applied electric field, **E**. Nonpolar molecules get polarized and thus behave as localized stationary dipoles. The effects of the single dipoles cancel each other macroscopically inside the dielectric. However, no partners with opposite charges are present on the surfaces; these thus have a stationary charge, called a free charge $\mathbf{E_o}$. The free charge weakens the effective charge as follows,

$$\mathbf{E} = \frac{Eo}{\varepsilon r}$$

If **p** is the polarization vector, then the induced electric field $\mathbf{E_p}$ will be in opposite direction to the applied force.

Whereby

$$\mathbf{E_p} = \mathbf{E_o} - \mathbf{E}$$
$$= \frac{\varepsilon r - 1}{\varepsilon r} \mathbf{E_o}$$
$$= \frac{p}{\varepsilon o}$$

Also on the introduction of a dielectric between any parallel plate capacitor, the capacitance can become expressed as

$$\mathbf{C_{dielectric}} = \varepsilon_r \varepsilon_o \frac{A}{d}$$

Thus introducing the voltage across the charged plates, **V**, the quantity of charge across the plates can be expressed as

$$\mathbf{Q} = \varepsilon_r \varepsilon_o \frac{A}{d} \mathbf{V}$$

Having established all parameters, the dielectric constant of the medium can be expressed as

$$\varepsilon_r = \frac{1}{\varepsilon o} \frac{d}{A} \cdot \frac{Q}{V}$$

2.4 CRYSTALLIZATION OF ZIRCONIUM OXIDE

Studies on the crystallization of ZrO_2 has attracted a lot of attention from many researchers. From the point of view of the present thesis work, in is important to remember, that at atmospheric pressure, zirconium oxide may possess three known crystallographic phases - monoclinic, tetragonal, and cubic, whereby the tetragonal and cubic phases are called high-temperature phases, which should be stable in the bulk form at temperatures exceeding 1000 Celsius degrees. At room temperature, if apparent, the cubic and tetragonal ZrO_2 are called metastable phases of zirconia.

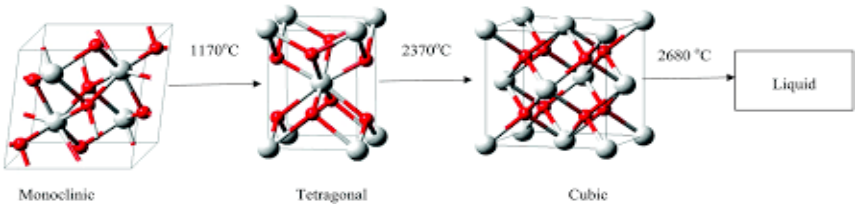

Figure 2 - The three crystallographic phases of Zirconium Oxide. Adapted from https://pubs.rsc.org/en/content/articlehtml/2016/dt/c6dt03484e

Although all the ZrO_2 phases are represented as zirconium dioxides, the real stoichiometry in the synthesized materials such as deposited films is deviated, mainly due to the large amounts of oxygen vacancies. The zirconia is characterized by varying amounts of vacancies, enhanced by dopants, which can modify the dielectric behavior of the material [Yldirim and Pachter, 2019, ACS Appl. Electr. Mater.]. The cubic and tetragonal phase formation actually can take place due to the existence of oxygen vacancies introduced by doping with metals of different valences. For instance, stabilization of cubic ZrO_2 after doping with yttrium (Y) has been realized by atomic layer deposition, and studied as a useful effect before application in memory capacitors, because cubic phase is characterized by markedly higher dielectric permittivity compared to the monoclinic phase [Park, 2017, J. Alloys Compd.].

Considering the thermal instability of cubic and/or tetragonal zirconium oxide metastable phases at room temperature and temperatures below 1000 degrees, it is essential to introduce the proper dopant during the deposition of pure ZrO_2 [Gehensel, 2021, J. Eur. Ceram. Soc.] The controlled insertion of dopants may turn out quite challenging, especially in nanomaterials.

Generally, the cubic and/or tetragonal phases of ZrO_2 can quite easily be formed in very thin films grown by atomic layer deposition method. The metastable phases may feasibly become formed, because the very thin films are quite naturally nanocrystalline, and thus full of defects, primarily oxygen vacancies. However, these metastable phases may become turned to the stable monoclinic phase upon heat treatments and, therefore, doping with other metal oxides, such as aluminum oxide, is recommended, as the introduction of foreign metal oxide layers (Al_2O_3) enables keeping the crystallite size in the main material (ZrO_2) low enough. Smallest possible crystallites are the most stable against phase transformation from cubic to monoclinic during heat treatments and other possible post-deposition procedures. It must be noted, that in accord with earlier reports, permittivity values up to 35 were achieved in about 10 nm thick trilayer ZrO_2-Al_2O_3-ZrO_2 films atomic layer deposited specifically for the application in DRAM cells [Knebel, 2014, IEEE Transact.].

2.5 ATOMIC LAYER DEPOSITION AND GROWTH OF DOPED ZIRCONIUM OXIDE

Atomic layer deposition is a chemical thin film deposition method based on sequential, self-saturating surface reactions. Certain precursor chemicals containing component elements for the target compound materials are introduced at different intervals, alternately, into the reactors. During ALD processes, inert gas flows are used as both precursor carriers as well as for evacuating the excess precursors and gaseous reaction products from the reaction chamber. ALD was first introduced by Dr. Tuomo Suntola at around 1970 to enable production of thin-film electroluminescent flat panel displays for computers, and is currently been used in the production of processors and memory chips, in development of semiconductor manufacturing, as well as in several more applications [Ritala and Niinistö, 2009, ECS Transact.]. Possibly, the only limitation to ALD is the intrinsic necessity to grow materials layer by layer, i.e., via the deposition cycles which leads to extended deposition

time that may be incompatible with large scale production if coatings with thicknesses higher than 1-20 nm are needed.

Atomic layer deposition is thus a nanotechnology-based deposition process employed for coating very thin films on any shape and geometry. The two distinct characterization of atomic layer deposition include highly conformal coating and self-limiting atomic layer by layer growth. Within the present thesis work, the most important features of ALD have been the ability to grow films, uniform in thickness, on planar (two-dimensional) substrates with monolayer precision and the ability to dope the main dielectric oxide (ZrO_2) films usefully with smaller amounts of Al_2O_3, just by alternately layering larger numbers of ZrO_2 deposition cycles and small numbers of Al_2O_3 deposition cycles.

To grow ZrO_2 in the laboratory of thin film technology by ALD, and in order to prepare samples analysed in the present thesis work, the precursor of zirconium was zirconium tetrachloride, $ZrCl_4$ [Kukli, 2002, J. Appl. Phys.] and water was used as the oxygen source. Trimethylaluminum, $Al(CH_3)_3$, was applied as for the aluminum precursor, analogously to the processes earlier been established for thicker ZrO_2-Al_2O_3 films relevant to the evaluation of the mechanical performance of doped zirconia [Piirsoo, 2021, AIP Adv.]. The ALD procedure was carried out in a research scale flow-type hot wall reactor, where the set up consists of a stainless steel tube placed in a furnace [Arroval, 2016, Thin Solid Films]. A rotary vane vacuum pump was used to remove unreacted precursors and reaction by-products from the reaction chamber. The sample consisting of Al_2O_3 doped ZrO_2 films was deposited in an in-house built hot-walled flow-type ALD reactor at 300°C. The thin films were deposited on fractions of Si(100) wafers with a resistivity of 0.014–0.020 Ω·cm. The Si was boron-doped to the concentrations of up to 5×10^{18} –1×10^{19}/cm^3, and coated with 10nm thick crystalline TiN layer as shown below.

2.6 X-RAY DIFFRACTOMETRY

X-ray Diffractometry (XRD) is a method for determination of the crystal structure of ordered materials. It enables verification of the phase composition of thin film samples [Pandey, 2021, J. Mater. Sci.: Mater. Electron.], providing information on the intensity of crystallization, different possible phases of the same compound, and preferred crystallographic orientation, if present. X-Ray diffraction is basically an elastic scattering of incident X-ray beam without loss of photon energy, giving rise to increasing reflection intensities as material more ordered, in terms of better formed crystal lattice, is analyzed.

The XRD measurements relevant to the samples further electrically analysed in the present thesis work were conducted by Dr. Hugo Mändar. The films were examined using a diffractometer SmartLab™(Rigaku) implementing the grazing incidence X-ray diffraction (GIXRD) method and rotating Cu anode (λ = 0.15406 nm) working at 8.1 kW in a fixed incident angle (0.45°) mode.

2.7 ELLIPSOMETRY

An ellipsometer measures a change in the polarization of light as it reflects from a material medium with the measured response dependent on the optical properties and, often, thickness of each material layer constituting a multilayer stack [https://www.jawoollam.com/resources/ellipsometry-tutorial]. An important feature of ellipsometry is its ability to measure nanoscale layers used in microelectronics, semiconductors and data storage system. It can be applied for measuring dielectric materials, e.g., ZrO_2 [Yusoh, 2012, Proc. Eng.], semiconductor materials, and superconductor materials. The basic principle used in ellipsometry is the change in the polarization of light reflected from a sample surface been measured by taking measurement of amplitude ratio of two polarized light. By varying the angle of incidence the process can be repeated to get similar results and clearer understanding of both interfaces and surfaces of thin films been measured.

The spectroscopic ellipsometry measurements revealing the thicknesses of the samples were, prior to the electrical analysis, performed by Dr. Aarne Kasikov. To be able to measure the film thickness, optical measurements of the structures were performed using a microspot option where light is focussed on a film surface via a telescope. The converging angle of each beam was about 3° and the spot size about 0.35 × 0.8 mm for 65° angle of incidence. Fitting was performed using a program WinElli II. Fit quality was characterized using a correlation function between the measured and computed spectra R^2 reaching unity for optimum correspondence.

2.8. X-RAY FLUORESCENCE SPECTROMETRY

X-ray Fluorescence spectrometry (XRF) operates, based on the excitation of electrons in the sample atoms by high energy X-rays followed by the emission of characteristic photons with a certain energy, well correlated to the atomic number of each element [Sparks, 2004, Electrochim. Acta; Takahara, 2017, Rigaku J.]. This process can be carried out non-destructively such that the determination of the emitted characteristics helps in the smooth analysis of the process.

XRF is a microanalysis method which was used in the laboratory of thin film technology. Its samples could routinely be analyzed as received from the reactor chamber. The XRF measurements useful for the present thesis work were made by Mr. Peeter Ritslaid, using a wavelength dispersive x-ray fluorescence spectrometer ZSX-400 (Rigaku). The XRF analysis reveal the composition of the thin films in terms of relative concentrations of different metals, oxygen content and also that of some impurities, such as carbon. In addition, preliminary thickness values can be obtained.

2.9. TRANSMISSION ELECTRON MICROSCOPY

Transmission Electron Microscopy (TEM) is an advanced, but also one of the most expensive, method used for the characterization of nanomaterials. In TEM technique, an electron beam is used to transmit incident light via a thin foil. The electrons are later seen as scattered after interacting with the specimen. The ratio of the distance between the objective lens, the specimen and the image plane are considered as magnified by the lens [Yoo and Yang, 2015, Appl. Microscopy; Petford-Long, 2008, Annu. Rev. Mater. Res.]. The result shows primarily the degree of aggregation, the size of crystallites formed. Phase analysis is sometimes also possible, depending on the degree of lattice ordering.

Transmission electron microscopy of a selected sample further electrically analysed in the present thesis work was performed by Dr. Jekaterina Kozlova. The focused ion beam (FIB; FEI Nanolab 600 dual-beam (SEM-FIB) system) in situ lift-off technique was used to prepare thin samples for high-resolution transmission electron microscopy (HR-TEM) study. TEM analysis was performed in the scanning mode (STEM) at 200 kV using a Cs-probe-corrected transmission electron microscope (FEI Titan Themis 200).

The following **Figure 3** below represents the results of TEM studies on an exemplary grown and analysed within the present thesis work. The particular sample consisted of a stack of defective mixed buffer layer grown using five (5) $Zr_xAl_yO_z$ deposition cycles, which was followed by eighty (80) ZrO_2 deposition cycles. One can clearly see, that the TEM proves the crystalline nature of the sample film which was grown on crystalline titanium nitride (TiN) bottom electrode layer. The crystallinity is visualized and recognized as parallel lattice plane edges extending from lower interfaces to upper interfaces between layers of different compounds. The compound layers are also distinguished by elemental analysis enabled by the same TEM apparatus. Two lower and smaller panels in Figure 1 demonstrate the results of elemental profiling where the electrode layer containing titanium (Ti) and the functional ZrO_2 layer containing zirconium (Zr) can be clearly separated.

The ZrO_2:Al_2O_3 ($Zr_xAl_yO_z$) interface layer between TiN and ZrO_2 is not clearly distinguishable, due to its very low thickness. Its existence is just implied by certain amorphization of the TiN-ZrO_2 contact layer, as the junction between electrode and metal oxide dielectric does not look sharp and crystalline. In any case, the TEM imaging has visualized and proven the formation of dense and continuous (nano)crystalline dielectric insulator layer on (nano)crystalline bottom electrodes, ready for capacitance measurements.

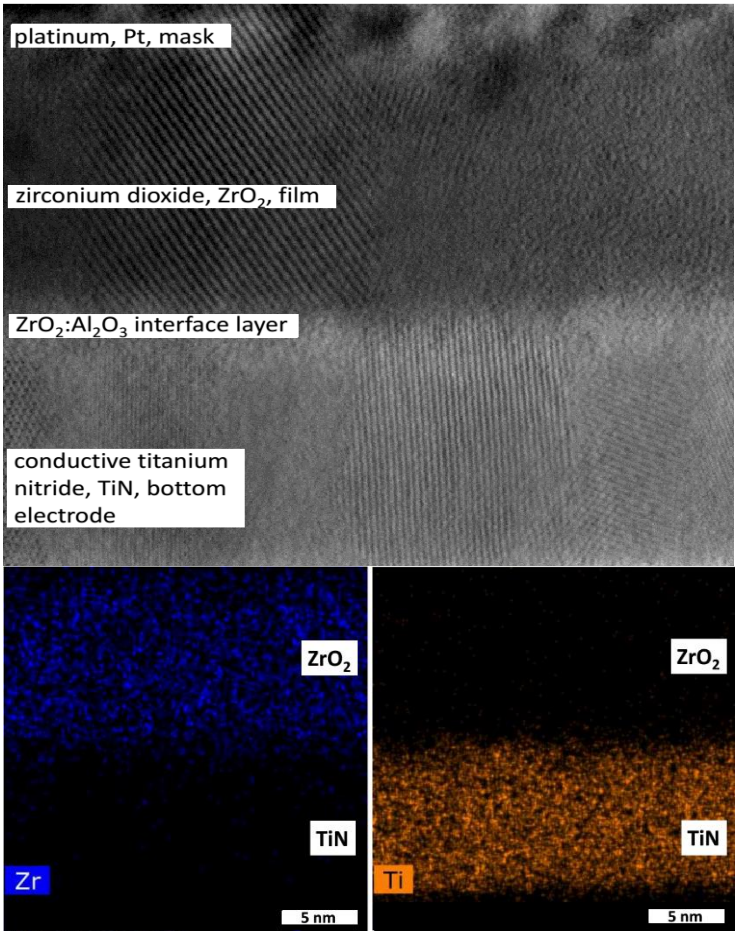

Figure 3 - Transmission electron microscopy (upper panel) and energy-dispersive X-ray spectroscopy (two lower panels) analysis results from stack of materials layers denoted by labels. The ZrO_2:Al_2O_3 interface layer between TiN and ZrO_2 was grown by ALD using a deposition cycle sequence of 5 × [$ZrCl_4$ + $Al(CH_3)_3$ + H_2O]. The ZrO_2 thin film was grown using a cycle sequence of 80 × ($ZrCl_4$ + H_2O). The analysis was performed by Dr. Jekaterina Kozlova.

3. RESULTS AND DISCUSSION: FILM GROWTH AND PERMITTIVITY

Prior to the capacitance measurements, carried out within the present thesis work, ZrO_2 and Al_2O_3 films were grown by atomic layer deposition on TiN-covered silicon substrates at the substrate temperature fixed at 300 ^{0}C. Two different metal precursors were used in the ZrO_2 and Al_2O_3 deposition processes, $ZrCl_4$ and $Al(CH_3)_3$, respectively, while H_2O was applied as the oxygen precursor. Purge periods were used after each oxidation step to enable pumping the non-reacted excessive precursors and gaseous reaction products (e.g., hydrogen chloride (HCl_4), methane (CH_4)) out of the reactor.

The reference ZrO_2 films were clearly crystallized. The reference Al_2O_3 films were, expectedly, amorphous. As was already revealed by the TEM image shown above, the ZrO_2 films grown on Al_2O_3-containing buffer layers were also definitely crystallized. The crystallinity depended somewhat on the content of the aluminum oxide dopant as will be explained further below.

Two different sample types were fabricated, based on different distributions of Al_2O_3 layers embedded by the host ZrO_2. In the first series, single Al_2O_3 deposition cycles were alternately deposited between ZrO_2 layers deposition using 2, 4, 9, 14, and 19 consecutive cycles of $ZrCl_4$ and H_2O, resulting in chemically periodic multilayers, in principle.

In the second series, an asymmetric structure was developed by first depositing mixed Al-Zr-O layers on the bottom TiN electrode, thus creating a chemically mixed and structurally more defective interfacial layer between the base TiN electrode and the host switching ZrO_2 medium. A single mixed layer was deposited after sequential exposure of the surface to $ZrCl_4$, $Al(CH_3)_3$, and H_2O pulses, without applying an oxidative water pulse between $ZrCl_4$ and $Al(CH_3)_3$. A homogeneous distribution of Zr and Al cations in the layer confined to the smallest possible thickness was targeted, aiming at the layered solid source of oxygen vacancies due to the difference in the valences of the two different metals mixed in the layer. The amount of single mixed interfacial layers deposited in sequence was varied between 1 and 5, always followed by the deposition of the main switching medium consisting of non-mixed ZrO_2. A reference sample was also deposited after application of 80 deposition cycles consisting of $ZrCl_4$, $Al(CH_3)_3$, and H_2O pulses.

The growth cycle sequences, thicknesses and elemental composition for both ZrO_2:Al_2O_3 and ZrO_2-$ZrAlO_x$ sample sets are presented in Tables **I** and **II**, respectively, below.

Table I. Growth cycles, thicknesses, and relative contents of elements contributing to ZrO_2:Al_2O_3 films initially programmed as periodical multilayers with uniform distribution of Al_2O_3 layers throughout the thickness of the host ZrO_2 film. The ranges of the atomic per cents, as presented, express the differences between measurement results obtained on different locations on substrate holder. Thickness was measured by ellipsometry. The elemental composition was determined by XRF.

ALD cycle sequences	Thickness	Al, at. %	Zr, at.%	O, at.%	Cl, at.%
$6\times(1\times Al_2O_3+24\times ZrO_2)$	14.6 nm	1.7-1.8	35.8-38.4	62.1-59.4	0.41-0.38
$30\times(1\times Al_2O_3+4\times ZrO_2)$	14.3 nm	9.0-8.7	25.9-31.4	64.7-59.5	0.41-0.44
$50\times(1\times Al_2O_3+2\times ZrO_2)$	16.1 nm	14.2-14.5	22.0-22.1	63.4-63.1	0.38-0.31
$150\times Al_2O_3$	19.95 nm	39.7-40.1	∅	60.3-59.9	∅
$120\times ZrO_2$	12.2 nm	∅	39.1-35.0	60.5-64.4	0.35-0.53

.

Table II. Growth cycles, thicknesses and relative contents of constituent elements, measured for about 1-2 nm thick ZrO_2-$ZrAlO_x$ films deposited on TiN substrates by applying sequential exposure of substrate surface to metal precursors without oxidizing steps between $ZrCl_4$ and $Al(CH_3)_3$, after which the main, 10-11 nm thick, ZrO_2 layer was deposited. Thickness was measured by ellipsometry. The elemental composition was determined by XRF.

ALD cycle sequences	thickness	Al, at. %	Zr, at.%	O, at.%	Cl, at.%
$1\times(ZrCl_4+TMA+H_2O)+80\times ZrO_2$	13.8 nm	1.4	25.6	72.7	1.3
$2\times(ZrCl_4+TMA+H_2O)+80\times ZrO_2$	10.6 nm	1.9	33.1	74.2	1.2
$3\times(ZrCl_4+TMA+H_2O)+80\times ZrO_2$	13.0 nm	0.5	27.4	68.5	0.8
$4\times(ZrCl_4+TMA+H_2O)+80\times ZrO_2$	12.1 nm	1.3	32.1	73.2	0.8
$5\times(ZrCl_4+TMA+H_2O)+80\times ZrO_2$	14.6 nm	1.2	31.0	72.2	0.8
$80\times(ZrCl_4+TMA+H_2O)$	10.7 nm	7.4	26.8	67.9	1.0

It is important to emphasize that the permittivity values measured and eventually considered in this study are based on multiple capacitive measurements carried out on at least ten (10) different Ti/ZrO_2:Al_2O_3/TiN capacitors chosen arbitrarily in a matrix of dot electrodes with area of 0.052 mm^2 laid over an area of 1 cm^2, approximately. After examining the capacitance dispersion on each single top electrode, the final curves were just averaged over the matrix.

Figure 4 represents single measurement results together with the averaged permittivity-frequency curves, calculated using the parallel-plate capacitor formula from each curve measured on a different capacitor. Despite an obvious scatter in the curves measured, the averaged values for non-doped ZrO_2 (Fig. 4, A) and Al_2O_3 films (Fig. 4, B), 30-31, and 10.5-10.6, respectively, are satisfactorily consistent with the known values characteristic of zirconium and aluminum oxides.

At measurement frequencies above 100 000 Hz (1E-5 Hz), the capacitance and related permittivity values started to decrease noticeably, which is probably indicative of the change from orientational (dipolar) charge polarization mechanism to the ionic one [See Figure 26, in: Wilk, Wallace, and Anthony, 2001, J. Appl. Phys. DOI: 10.1063/1.1361065]

Further, for the doped film deposited using 30 double cycles of ($1\times Al_2O_3$ + $4\times ZrO_2$). the permittivity within the flat value range varied from 15 to 30. For the doped film deposited using 6 double cycles of ($1\times Al_2O_3$ + $24\times ZrO_2$) the permittivity varied from 34 to 38. These films were deposited to the similar thicknesses (Table I). Hence, layering of Al_2O_3 alternately with more layers (24 versus 4 cycles) of ZrO_2 has given higher permittivity value. This was plausibly due to the better developed crystallization in the films, as will be discussed below in the next chapter.

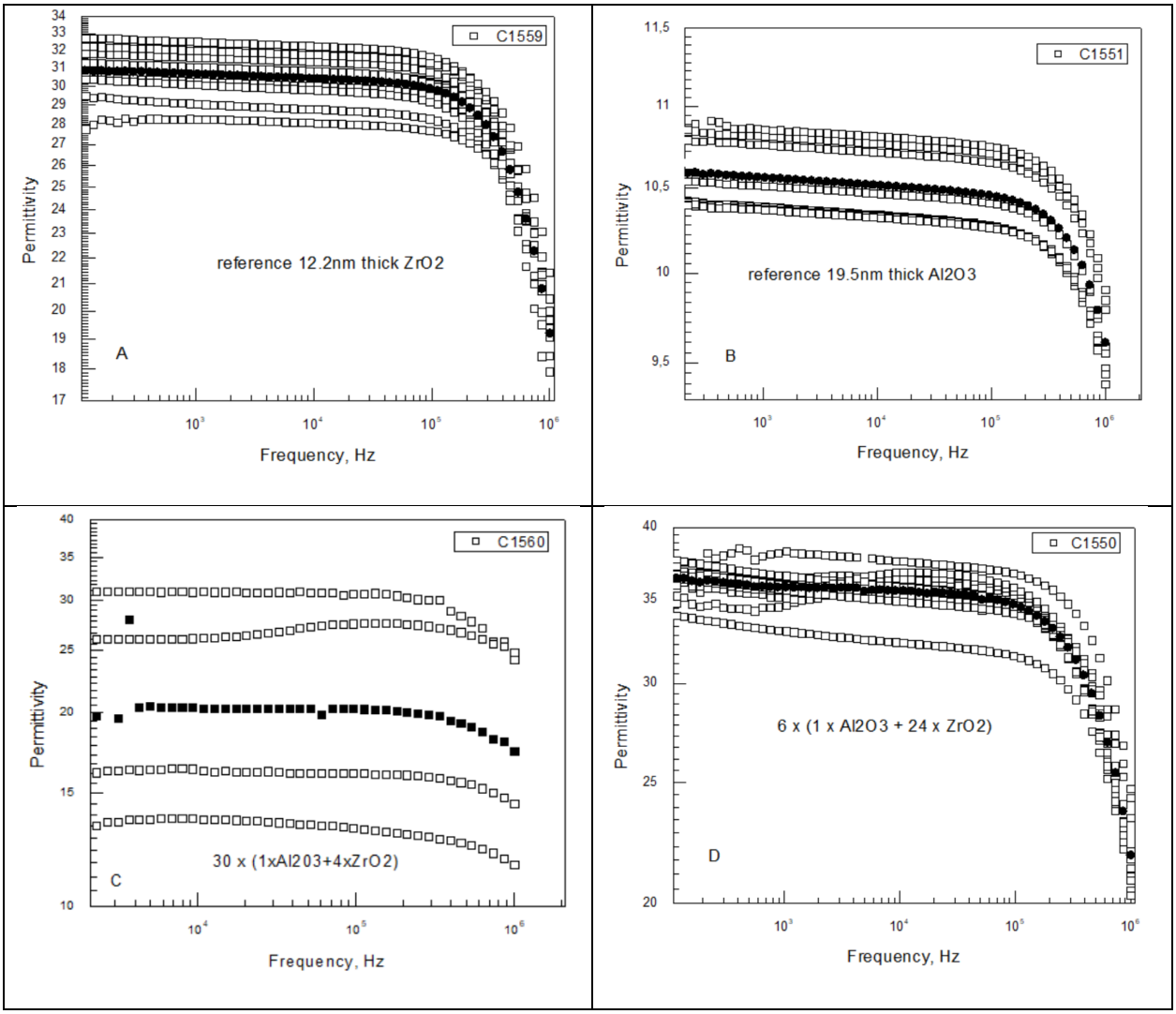

Figure 4 - Selected permittivity-frequency curves for reference ZrO_2 (A), reference Al_2O_3 (B), and Al_2O_3-doped ZrO_2 (C, D) films. The film growth cycle sequences for doped films are indicated by labels. Open squares denote single curves measured on separate top electrodes over the matrix. Black squares denoted the average values calculated over the set of measurements on corresponding electrode matrix.

Figure 5 below shows the permittivity variations in the films, where at first $Zr_xAl_yO_z$ buffer layers of mixed composition were deposited directly on TiN electrodes, and non-doped ZrO_2 films on such buffer layers (Fig. 5, A, B, C, D, F). Reference, thicker, film was deposited using the same cycle sequence as that for the $Zr_xAl_yO_z$ buffer, and electrically measured, too (Fig. 5, E). A closer look reveals how the permittivity curve remains almost flat below 100 000 Hz for all the samples, except that of the reference film. The average permittivity values can probably be related to the different degrees of crystal growth in the films, as will be discussed below in the next paragraph.

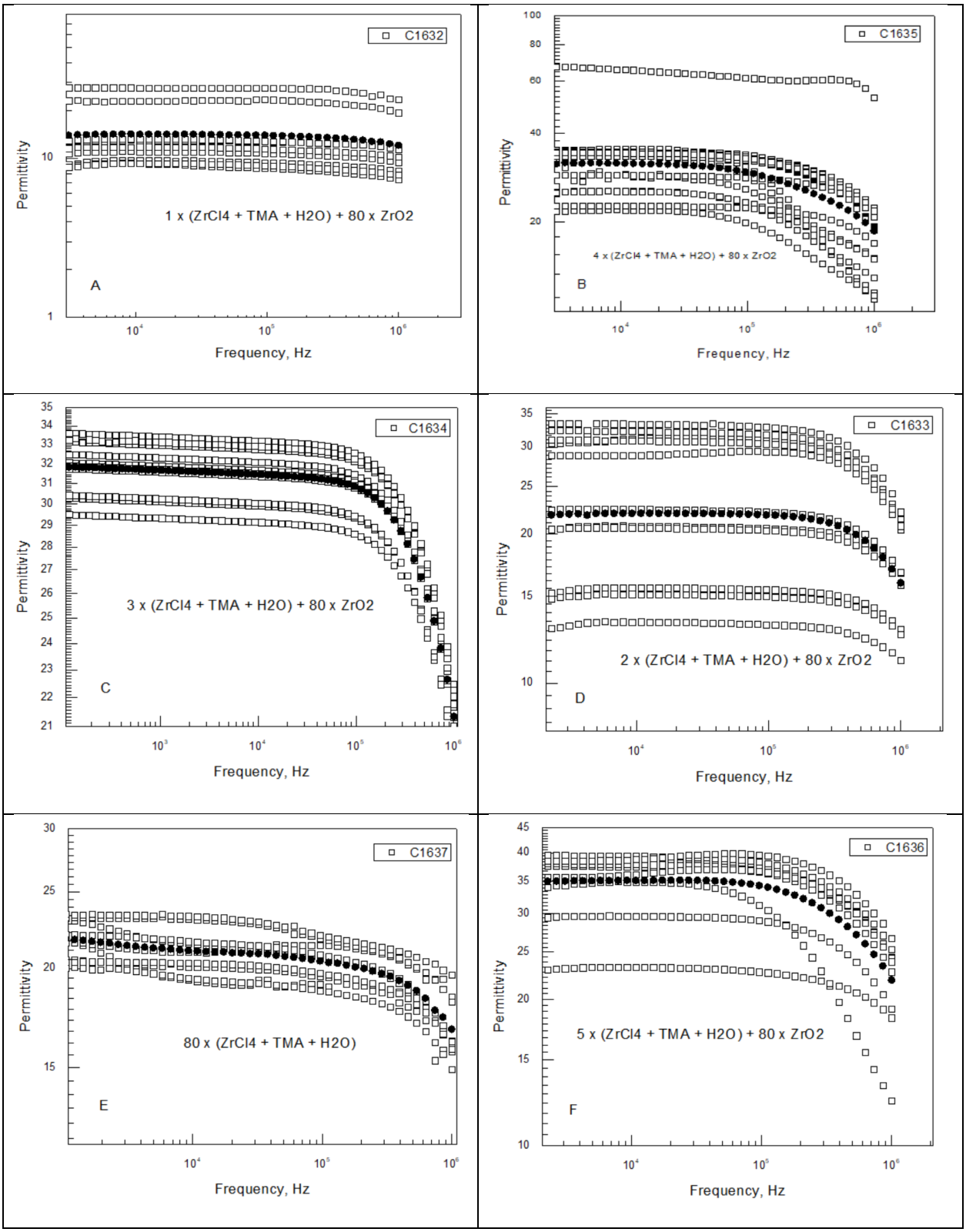

Figure 5 - Selected permittivity-frequency curves for ZrO_2 films grown on Al_2O_3-ZrO_2 mixed buffer layers. The film growth cycle sequences for doped films are indicated by labels. Open squares denote single curves measured on separate top electrodes over the matrix. Black squares denoted the average values calculated over the set of measurements on corresponding electrode matrix.

For reader's convenience and for the sake of clarity, the averaged permittivity *versus* measurement frequency curves can be presented comparatively in the following **Figure 6**.

In the case of reference Al_2O_3 and ZrO_2, as well as periodically layered 6× (1×Al_2O_3 + 24×ZrO_2) films, the capacitances could reliably be measured in the whole frequency range examined, and notably, down to the frequency values as low as 100 Hz (Fig. 6, a). This is indicative of successful deposition of well-insulating dielectric films. At the same time, in the case of periodically layered 30×(1×Al_2O_3 + 24×ZrO_2) film, the capacitance and accompanying permittivity became destabilized and non-measurable at about 5000 Hz, i.e., 5 kHz (Fig. 6, a). The reason was probably in the chemically more strongly mixed oxide composition and accompanying structural disorder resulting in higher density of electronic defects, causing interfacial polarization of charge carriers able to drift rather freely under applied voltage at low frequencies.

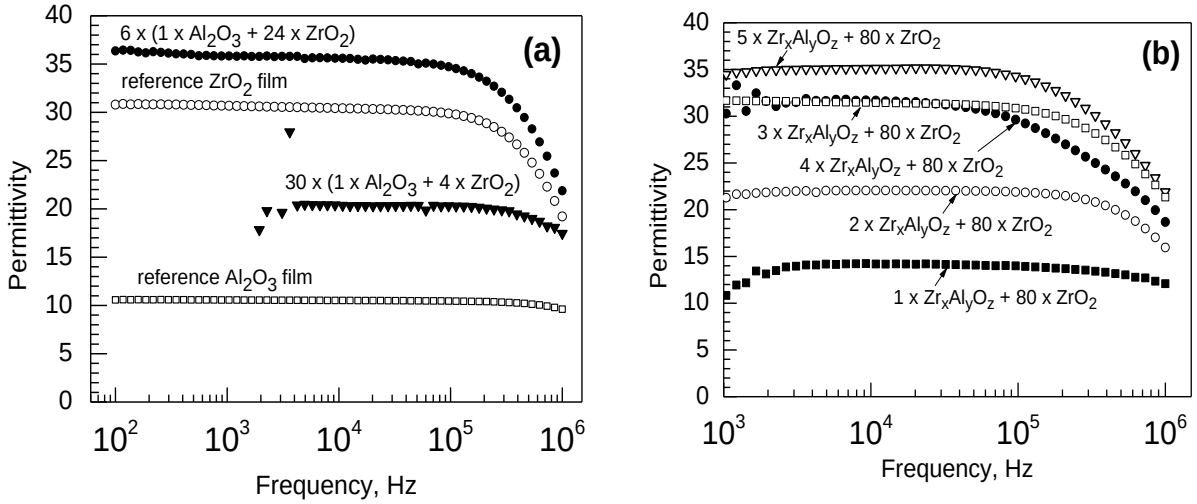

Figure 6. Averaged permittivity-frequency curves for periodically Al_2O_3-doped ZrO_2 films (a) and ZrO_2 films grown on Al_2O_3-ZrO_2 ($Zr_xAl_yO_z$) mixed buffer layers (b). The film growth cycle sequences for doped films are indicated by labels (a). Also indicated are the amounts of $Zr_xAl_yO_z$ growth cycles (b), where $Zr_xAl_yO_z$ denotes a cycle consisting of $ZrCl_4$ pulse, followed by $Al(CH_3)_3$ pulse, terminated by H_2O pulse. For the films composition and thicknesses, see Tables I and II.

In the case of non-doped ZrO_2 films grown on $Zr_xAl_yO_z$ buffer layers of mixed composition on TiN electrodes (Fig. 6, b), the capacitance became rather unstable in all samples at frequencies around 1000 Hz, i.e. 1 kHz, without clear systematic dependence on the amount of $Zr_xAl_yO_z$ buffer deposition cycles. The capacitive behavior of $Zr_xAl_yO_z$ reference film (Fig. 5, E), differed from the rest of samples in the series by its instabilities over the whole examined frequency range. In further regard with the rest of the samples, the average permittivity tended to increase with the amount of the $Zr_xAl_yO_z$ buffer deposition cycles in the row of 1, 2, 3, 4, and 5. The observation may at least partially become explained by the influence of crystallization, as will be pointed out below in the next chapter.

4. Relationship between film structure and dielectric behavior

Figure 7 depicts diffraction pattern taken from the 14.6 nm thick ZrO_2:Al_2O_3 sample. The latter sample was deposited in a periodical manner, that is, by double layering twenty-four (24) ZrO_2 ALD cycles alternately with one (1) Al_2O_3 cycle, for 6 times. One can clearly see, that the ZrO_2:Al_2O_3 films have become clearly crystallized. Since the film thickness is sufficiently low, the material is nanocrystalline, as also indicated by the low intensity and large width of the reflections.

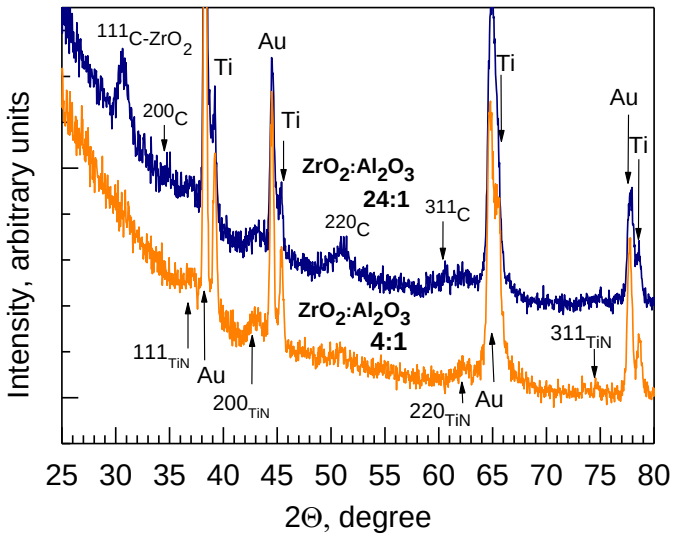

Figure 7 X-ray diffraction patterns measured from periodically layered ZrO_2:Al_2O_3 films grown using ALD cycle ratios of 24:1 (upper pattern) and 4:1 (lower pattern). The oxide films were deposited on titanium nitride (TiN) electrode substrates and supplied with top electrodes consisting of titanium (Ti) and gold (Au) stacks, before the XRD measurements. The reflections from bottom electrodes are denoted by Miller indexes belonging to cubic TiN (subscript TiN). The reflections from top metal electrodes are designated with the labels Ti and Au. The reflections from the main solid oxide medium are assigned as belonging to cubic (subscript C) ZrO2 with corresponding Miller indexes. The patterns were recorded by Dr. Hugo Mändar.

Figure 7 also depicts diffraction pattern taken from the 14.3 nm thick ZrO_2:Al_2O_3 sample deposited by double layering our (4) ZrO_2 ALD cycles alternately with one (1) Al_2O_3 cycle, for 30 times. One can see, that, besides the strong reflection peaks arising from the top metal electrodes (Ti and Au) and weak reflections from the bottom TiN electrodes, no reflections could be attributed to the ZrO_2:Al_2O_3 film. This means that the oxide medium remained X-ray amorphous. This can be explained by relatively high aluminum content doped into the ZrO_2. The content of Al, measured by X-ray fluorescence spectrometry, was 8.7-9.0 atomic % in the amorphous film deposited using ZrO_2:Al_2O_3 cycle ratio of 4:1, as compared to the 1.7-1.8 %, measured in the nanocrystalline film deposited using ZrO_2:Al_2O_3 cycle ratio of 24:1. The high content of aluminum in the former film was

sufficient for the complete destruction of crystallographic order, whereas in the latter film the content of aluminum was chosen appropriately, allowing formation of metastable (likely cubic) lattice.

Importantly, the differences in the degrees of ordering determined the capacitive behavior characteristic of the Au/Ti/ZrO_2:Al_2O_3/TiN/Si/Al capacitors based on ZrO_2:Al_2O_3 dielectric insulators. The average dielectric permittivity calculated from the capacitance-frequency curves of the sample with metastabilized cubic ZrO_2:Al_2O_3 film reached 36 (Figure 4, D). At the same time, the average permittivity of the amorphous ZrO_2:Al_2O_3 film remained, expectedly, lower, approximately at 20 (Figure 4, C). It is worth further noting that the average permittivity of non-doped 12.2 nm ZrO_2 film was approximately 30 and the permittivity of 19.5 nm thick Al_2O_3 film reached 10.5. Essentially, these values satisfactorily resemble those earlier reported for the respective phases and compounds, as was reviewed above.

Figure 8 demonstrates diffraction patterns taken from the 12.2 nm thick reference ZrO_2 film (topmost pattern) and also from the 10.7 nm thick ZrO_2-Al_2O_3 mixed reference film (bottom pattern). The latter films were grown using ALD pulse-purge sequences of $ZrCl_4$ + purge + $Al(CH_3)_3$ + purge + H_2O + repeated for 80 times. One can clearly see, that the reference ZrO_2 film was crystallized in the form of either cubic or tetragonal polymorph, possibly as in a mixture of both metastable phases. At the same time, the mixed ZrO_2-Al_2O_3 film, which can also become denoted as $Zr_xAl_yO_z$, could not become ordered, as can be decided on the basis of the diffraction pattern lacking any reflections other than those arising from TiN bottom electrode layer. Thus, a completely X-ray amorphous material was deposited. Rather expectedly, the permittivity remained moderate, with average value reaching 22. Notably, and differently from the other permittivity-frequency curves measured in this work, the dispersion curves were lacking flat plateaus, exhibiting nonuniform behavior of capacitance against measurement frequency (Figure 5, E). Such a behavior may be indicative, besides structural disorder, also certain compositional inhomogeneities throughout the film, with increased defect densities. This film contained also relatively high amounts of aluminum up to 7.4 atomic %, although the content of zirconium was markedly higher, reaching 26.8 at.%.

The deposition of ultrathin mixed ZrO_2-Al_2O_3 films without oxidative H_2O pulse between zirconium and aluminum precursors (also can be denoted as $Zr_xAl_yO_z$) was, further, intentionally used as a potential source of electronic defects in the form of buffer layers deposited between bottom TiN electrodes and the main ZrO_2 solid films. This was done with further aims at the creation of films enabling stabilization of two different electronic conductivity states between bottom and top electrodes. Such behavior is called resistive switching. In order to initiate resistive switching effect, feasibly sourcing electronic current by means of some defect resevoirs can become beneficial. The investigation of the resistive switching behavior remains beyond the scope of the present thesis work. Never the less, it became necessary to study capacitive behaviour of the potentially switching media, because the relationship between film structure, capacitance, and related permittivity values, may in general be regarded as a pre-requisite before estimation of the stability of electronic devices.

In this connection**, Figure 8** shows also patterns belonging to such samples grown by ALD by first depositing mixed ZrO_2-Al_2O_3 ($Zr_xAl_yO_z$) buffer layers directly onto titanium nitride (TiN) substrate electrode. The amount of pulse-purge sequences of $ZrCl_4$ + purge + $Al(CH_3)_3$ + purge + H_2O was repeated by N times indicated by the corresponding labels at the patterns. The deposition of such buffer layers was in all cases followed by deposition of 10-14 nm thick ZrO_2 films, not mixed with Al_2O_3, using 80 ALD cycles consisting of $ZrCl_4$ pulse – purge – H_2O pulse – purge periods. The capacitor structures devised are schematically described in **Figure 9**.

The deposition of ultrathin mixed $Zr_xAl_yO_z$ buffer layers had an obvious effect to the relationship between permittivity of the $Zr_xAl_yO_z$-ZrO_2 stacked layers and the amount of $Zr_xAl_yO_z$ deposition cycles. Partially, the relationship can be supported and may become explained by the accompanying changes in the intensity of crystallization in these films. At first and somewhat surprisingly, the film containing buffer layer deposited after only one (N = 1) $Zr_xAl_yO_z$ cycle possessed average permittivity not exceeding 12 (Figure 5, A), although the film was apparently clearly crystallized, exhibiting strong reflections from the metastable ZrO_2 (**Figure 8**, the second pattern from bottom).

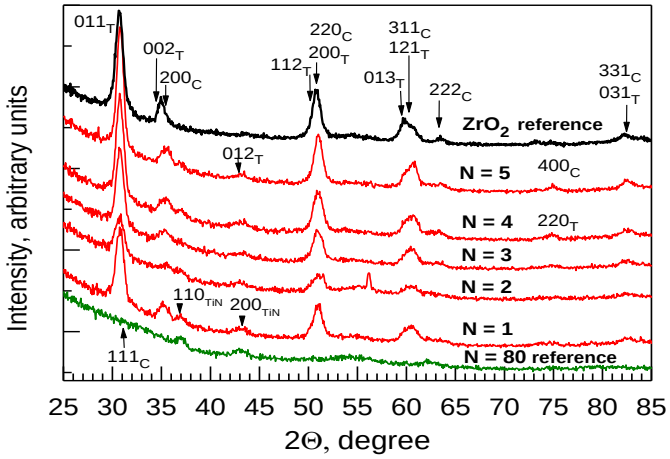

Figure 8 X-ray diffraction patterns measured from the reference ZrO_2 film (top pattern), and layered ZrO_2:Al_2O_3 films grown using 80 ALD cycles in alternating sequences of [$ZrCl_4$ pulse + purge + $Al(CH_3)_3$ pulse + purge + H_2O pulse + purge] (bottom pattern). The patterns depicted between the topmost and bottom ones depict those from films grown using ALD cycle sequences of N × [$ZrCl_4$ pulse + purge + $Al(CH_3)_3$ pulse + purge + H_2O pulse] + 80 × ($ZrCl_4$ pulse + purge + H_2O pulse + purge), with N as integer increasing from bottom to top. The reflections from the main solid oxide medium are assigned as belonging to either cubic (subscript C) or tetragonal (subscript T) ZrO_2 with corresponding Miller indexes. Also indicated are the reflections from crystalline cubic TiN eleectrode. The patterns were measured from the films without top Au/Ti metal electrodes. The patterns were recorded by Dr. Hugo Mändar.

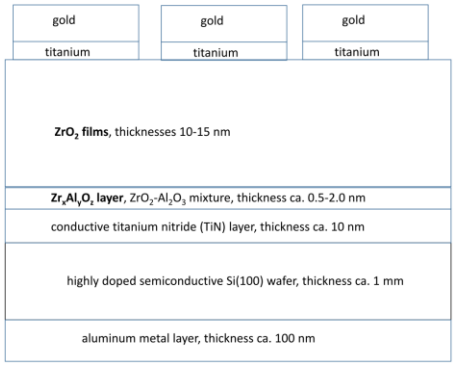

Figure 9 Schematic representation of the capacitor stack formed after deposition of ultrathin mixed ZrO_2-Al_2O_3 films without oxidative H_2O pulse between zirconium and aluminum precursors (also denoted as $Zr_xAl_yO_z$) as buffer layer between bottom TiN electrodes and the main ZrO_2 solid films. The layer thicknesses are not to scale.

Further, in the series of films containing buffer layers grown using 2-5 $Zr_xAl_yO_z$ deposition cycles the permittivity tended to increase with the number of the cycles. The averaged permittivity values reached 22, 32, 32, and 35, for the films on buffer layers grown using 2, 3, 4, and 5 $Zr_xAl_yO_z$ deposition cycles, respectively (Figure 5, B, C, D, F). This might be connected to the development of crystallinity which is expressed by the intensifying or sharpening the reflections attributed to metastable tetragonal phases of ZrO_2. The reflections (**Figure 8**) are those indexed as 101, 002, 012, 112, 013, and 031, at 2Θ values of 30.3, 34.7, 43.1, 50.4, 59.5, 60.4, and 82.8 degrees, respectively, for the oxygen-deficient metastable tetragonal ZrO_2 polymorph (X-ray diffraction card 96-210-0389, $Zr_{2.00}O_{3.94}$).

Increase in the permittivity together with the formation and intense nanocrystallization of ZrO_2 phases of higher permittivity than that characteristic of normally stable ZrO_2 may not be surprising, but can in certain limits become controlled by choice of the deposition recipes. However, the evident increase in the permittivity, as well as the possible advancement in film structure upon just increasing the number of buffer $Zr_xAl_yO_z$ layer deposition cycles, are both even more interesting phenomena, which remain not fully explained at this stage of study.

SUMMARY AND CONCLUSIONS

This study has revealed that electrically adequately performing ZrO_2 and Al_2O_3 thin films can effectively be combined in layered mixtures and stacks synthesized using atomic layer deposition technique from zirconium tetrachloride and trimethylaluminum precursors. Stacked layers (or nanocomposites) consisting of ZrO_2 and Al_2O_3 have shown advanced properties compared to their single constituents separately. This is because in the nanolayered composites the useful physical properties of both oxides could effectively be tailored. ZrO_2 provided high dielectric permittivity even in structurally strongly disordered state, whereby Al_2O_3 assisted in stabilization of metastable high-permittivity ZrO_2 phases. In addition, Al_2O_3 could assist in reduction of leakage through the insulating dielectric layer because of its wider band-gap. Secondly, exposure of the substrate to variable amounts of the precursors and forming oxide layers could significantly improve the average structural uniformity and hence the dielectric strength. This is because the excessive growth of crystallites and grain boundaries of zirconium oxide was interrupted by the introduction of intermediate amorphous aluminum oxide layers.

Thus, by varying the number of growth per cycle via changing the contents of the component compounds, the physical properties of ZrO_2 and Al_2O_3 were controlled and desirable results were obtained. Regarding the composition of the solid films deposited in periodical manner, it was noticed that the most stable capacitive behavior together with the highest relative permittivity values were achieved in the ZrO_2-based films containing less than 2 atomic per cents of aluminum (oxide). Increasing the content of aluminum close to 10 atomic per cents brought about twofold decrease in the permittivity, from ca. 38 to 20, plausibly due to the excessive amorphization of the structure, as was decided on the basis of featureless X-ray diffraction patterns.

In regard with the deposition of ZrO_2 and Al_2O_3 in the stacked combinations, where the main ZrO_2 films were grown on ultrathin ZrO_2-Al_2O_3 buffer layers, even more interesting results were obtained. The permittivity of the stacked films obviously increased with the increased amount of the buffer layer deposition cycles, which requires further studies before one could provide full explanation.

After summarizing the results, one can conclude that it is evidently possible to tune the capacitive properties of thin ZrO_2-Al_2O_3 films by modifying the sequence of atomic layer deposition cycles. Moreover, the capacitance and therewith the effectively averaged dielectric permittivity can depend, besides dopant-induced changes in the internal structural order of solid medium, also on modifications of the contact layers between the dielectric insulator film and electrodes. The capacitive polarization in the materials, and their structure-related permittivity, probably correlate to their insulating properties, as well. This will likely be connected to the resistive switching effects demonstrated by the same materials. The capacitance and permittivity values obtained during the present thesis work turned out as useful, will add to the knowledge and will be reported in the manuscript of a scientific article under preparation, to be published in scientific literature,

written by Joonas Merisalu and colleagues, and provisionally titled as “Structure and electrical properties of zirconium aluminum oxide thin films engineered by atomic layer deposition.” The latter paper will be devoted to the resistive switching behavior of ZrO_2-Al_2O_3 thin films.

REFERENCES

1) Abbas. Y, Han. I. S, Sokolov. A. S, Jeon. Y.-R, Choi. C, 2020 Rapid thermal annealing on the atomic layer-deposited zirconia thin film to enhance resistive switching characteristics, J Mater. Sci.: Mater. Electr. 31, 903–909.
2) Arroval. T, Aarik. L, Rammula. R, Kruusla.V, Aarik. J, 2016, Effect of substrate-enhanced and inhibited growth on atomic layer deposition and properties of aluminum–titanium oxide films, Thin Solid Films 600, 119–125.
3) Castán. H, Dueñas. S, Kukli. K, Kemell. M, Ritala. M, Leskelä. M, 2018, Study of the influence of the dielectric composition of Al/Ti/ZrO_2:Al_2O_3/TiN/Si/Al structures on the resistive switching behavior for memory applications, ECS Transact. 85, 143.
4) Cho. H. J, Kim. Y. D, Park. D. S, Lee. E, Park. C. H, Jang. J. S, Lee. K. B, Kim. H. W, Chae. S. J, Ki. Y. J, Han. I. K, Song. Y. W, 2006, New TIT Capacitor with ZrO_2/Al_2O_3/ZrO_2 dielectrics for 60nm and below DRAMs, published in 2006 European Solid-State Device Research Conference http://dx.doi.org/10.1109/ESSDER.2006.307659.
5) Cho. H. J, Kim. Y. D, Park. D. S, Lee. E, Park. C. H, Jang. J. S, Lee. K. B, Kim. H. W, Chae. S. J, Ki. Y. J, Han. I. K, Song. Y. W, 2007, New TIT Capacitor with ZrO_2/Al_2O_3/ZrO_2 dielectrics for 60nm and below DRAMs, Solid-State Electronics 51, 1529–1533.
6) Clark. R.D, 2014, Emerging applications for high K materials in VLSI technology, Materials, 7, 2913-2944; http://dx.doi.org/10.3390/ma7042913.
7) Gehensel. R.J, Zierold. R, Schaan. G, Shang. G, Petrov. A.Y, Eich. M, Blick. R, Krekeler. T, Janssen. R, Furlan. K. P, 2021, Improved thermal stability of zirconia macroporous structures via homogeneous aluminum oxide doping and nanostructuring using atomic layer deposition, J. Eur. Ceram. Soc. 41, 4302–4312.
8) Grove. T. T, Masters. M. F, Miers. R. E, 2005, Determining dielectric constants using a parallel plate capacitor, Am. J. Phys. 73, 52.
9) Harrop. P.N, Wanklyn. J.N, 1967, The dielectric constant of zirconia, Br. J. Appl. Phys. 18, 739-742.
10) Hausmann. D. M, Kim. E, Becker. J, Gordon. R. G, 2002, Atomic layer deposition of hafnium and zirconium oxides using metal amide precursors, Chem. Mater. 14, 4350 – 4358.
11) Hua. Q, Wu. H, Gao. B, Zhao. M, Li. Y, Li. X, Hou. X, Chang. M-F, Zhou. P, Qian. H, 2019, A threshold switching selector based on highly ordered Ag nanodots for X-point memory applications, Adv. Sci. 6, 1900024. http://dx.doi.org/10.1002/advs.201900024.
12) Huang. A.p, Chu. K.p, Yan. H, Zhu. M. K, 2005, Dielectric properties enhancement of ZrO_2 thin films induced by substrate biasing, J. Vac. Sci. Technol. 23, 566-569.

13) Hwang. C.-S, Yoo. C. Y, editors, 2014, Atomic layer deposition for semiconductors, Springer Science + Business Media, New York http://dx.doi.org/10.1007/978-1-4614-8054-9.
14) Kahro. T, Castán. H, Dueñas. S, Merisalu. J, Kozlova. J, Jõgiaas. T,Piirsoo. H.-M, Kasikov. A, Ritslaid. P, Mändar. H, Tarre. A, Tamm. A, Kukli. K, 2020, Structure and behavior of ZrO_2-graphene-ZrO_2 stacks, J. Vac. Sci. Technol. A 38, 063411.
15) Knebel. S, Schroeder. U, Zhou. D, Mikolajick. T, Krautheim. G, 2014, Conduction mechanisms and breakdown characteristics of Al_2O_3-doped ZrO_2 high-k dielectrics for three-dimensional stacked metal–insulator–metal capacitors, IEEE Transact. Dev. Mater. Reliab. 14, 154-160. https://doi.org/10.1109/TDMR.2012.2204058.
16) Kukli. K, Niinistö. J, Tamm. A, Lu. J, Ritala. M, Leskelä. M , Putkonen. M, Niinistö. L, Song. F, Williams. P, Heys. P.N, 2007, Atomic layer deposition of ZrO_2 and HfO_2 on deep trenched and planar silicon, Microel. Eng. 84, 2010–2013.
17) Kukli. K, Ritala. M, Aarik. J, Uustare. T, Leskelä. M, 2002, Influence of growth temperature on properties of zirconium dioxide films grown by atomic layer deposition, J. Appl. Phys. 92, 1833-1840.
18) Panda. D, Tseng. T.-Y, 2013, Growth, dielectric properties, and memory device applications of ZrO_2 thin films, Thin Solid Films 531, 1–20.
19) Pandey. A, Dalal. S, Dutta. S, Dixit. A, 2021, Structural characterization of polycrystalline thin films by X-ray diffraction techniques, J. Mater. Sci.: Mater. Electron. 32, 1341–1368. https://doi.org/10.1007/s10854-020-04998-w.
20) Park. B.-E, Oh. I.-K, Mahata. C, Lee. C. W, Thompson. D, Lee. H.-B.-R, Maeng. W. J, Kim. H, 2017, Atomic layer deposition of Y-stabilized ZrO_2 for advanced DRAM capacitors, J. Alloys Compd. 722, 307-312.
21) Petford-Long. A. K, Chiaramonti. A. N, 2008, Transmission electron microscopy of multilayer thin films, Annu. Rev. Mater. Res. 38, 559–584. https://doi.org/10.1146/annurev.matsci.38.060407.130326.
22) Piirsoo. H.-M, Jõgiaas. T, Mändar. H, Ritslaid. P, Kukli. K, Tamm. A, 2021, Microstructure and mechanical properties of atomic layer deposited alumina doped zirconia, AIP Adv. 11, 055316. https://doi.org/10.1063/5.0047572.
23) Ritala. M, Niinistö. J, 2009, Industrial applications of atomic layer deposition, ECS Transact., 25, 641-652. https://doi.org/10.1149/1.3207651.
24) Sparks. C. M, Beebe. M. R, Bennett. J, Foran. B, Gondran. C, Hou. A, 2004, Characterization of high-k gate dielectric and metal gate electrode semiconductor samples with a total reflection X-ray fluorescence spectrometer, Spectrochim. Acta B 59. 1227–1234.
25) Takahara. H, 2017, Thickness and composition analysis of thin film samples using FP method for XRF analysis, Rigaku J. 33, 17-21. https://pcsanalytika.cz/wp-content/uploads/2019/07/Rigaku_Journal_01-Thin-film-analysis.pdf.

26) Wilk. G. D, Wallace. R. M, Anthony. J. M, 2001, High-k gate dielectrics: Current status and materials properties considerations, J. Appl. Phys. 89, 5243-5275.

27) Wintgens. C, The 50-nm DRAM battle rages on: An overview of Micron's technology, 2009, https://www.eetimes.com/the-50-nm-dram-battle-rages-on-an-overview-of-microns-technology/# (last accessed December 29, 2021).

28) Xie. J, Zhu. Z, Tao-H, Zhou. S, Liang. Z, Li. Z, Yao. R, Wang. Y, Ning. H, Peng. J, 2020, Research progress of high dielectric constant zirconia-based materials for gate dielectric application, Coatings, 10, 698.

29) Yildirim. H, Pachter. R, 2019, Extrinsic dopant effects on oxygen vacancy formation energies in ZrO_2 with implication for memristive device performance, ACS Appl. Electron. Mater. 1, 467−477.

30) Yoo. J. H, Yang. J.-M, 2015, Cross-sectional transmission electron microscopy specimen preparation technique by backside Ar ion milling, Appl. Microsc. 45,189-194. http://dx.doi.org/10.9729/AM.2015.45.4.189.

31) Yusoh. R, Horprathum. M, Eiamchai. P, Chindaudom. P, Aiempanakit. P, 2012, Determination of optical and physical properties of ZrO_2 films by spectroscopic ellipsometry, Proc. Eng. 32, 745–751. https://doi.org/10.1016/j.proeng.2012.02.007.

32) Zhao. X, Vanderbilt. D, 2002, Phonons and lattice dielectric properties of zirconia, Phys. Rev. B, 65, 075105.

ACKNOWLEDGEMENTS

I would like to express my sincere gratitude and appreciation to my supervisor Kaupo Kukli, PhD for the willingness to help, for the support and above all the opportunity of letting me conduct this research. I am also thankful for the experience I have received under the supervision of Joonas Merisalu, Msc for taking the time to share his knowledge with me and providing continuous insightful guidance and advice throughout my time under his supervision.
I wish to send my gratitude to my family for their contribution throughout my academic period.

Non-exclusive licence to reproduce the thesis and make the thesis public

I, CHINEDU HENRY OFOEGBU

_____,

(*author's name*)

1. grant the University of Tartu a free permit (non-exclusive licence) to reproduce, for the purpose of preservation, including for adding to the DSpace digital archives until the expiry of the term of copyright, my thesis

CAPACITIVE BEHAVIOUR OF ATOMIC LAYER DEPOSITED NANOMATERIALS FOR MEMORIES

_____,

(*title of thesis*)

supervised by KAUPO KUKLI, PhD and JOONAS MERISALU, MSc

_____.

(*supervisor's name*)

2. I grant the University of Tartu a permit to make the thesis specified in point 1 available to the public via the web environment of the University of Tartu, including via the DSpace digital archives, under the Creative Commons licence CC BY NC ND 4.0, which allows, by giving appropriate credit to the author, to reproduce, distribute the work and communicate it to the public, and prohibits the creation of derivative works and any commercial use of the work until the expiry of the term of copyright.
3. I am aware of the fact that the author retains the rights specified in points 1 and 2.
4. I confirm that granting the non-exclusive licence does not infringe other persons' intellectual property rights or rights arising from the personal data protection legislation.

Chinedu Henry Ofoegbu

18/01/2022